# A Phase Doppler System for High Concentration Sprays

Chris Fandrey, Amir Naqwi, Joseph Shakal and Hai Zhang

TSI Inc.

## ABSTRACT

Various peculiar aspects of drop sizing in a dense spray, using the phase Doppler technique, are considered. In order to ensure that only one drop exists in the probe volume at any given time, the laser beams need to be focused to a very small spot, such as 50 µm. This may lead to deviations from the normally assumed Gaussian beam optics on the transmitting side. Hence, theoretical estimates of the probe volume dimensions are not reliable and may lead to erroneous measurement of liquid volume flux. In this report, a method of experimentally qualifying the phase Doppler probe volume is described for accurate volume flux measurements.

The small probe volume results in the so-called trajectory effect becoming important; i.e. a dependence of the measurement upon the particle trajectory, some signals may be based predominantly on reflection mode of scattering instead of refraction. Simply processing these signals (or allowing them to be processed) results in incorrect drop diameter measurements. The challenge for the instrumentation developer is to not only eliminate these erroneous signals, but also collect good signals from a well-defined region in space, so that the measured data can be correctly reduced to liquid volume flux and droplet concentration.

The above objectives are achieved in this work using a combination of signal amplitude discrimination and phase-ratio discrimination. The signal amplitude based discrimination is further developed by introducing an automated procedure to find the intensity limits. This procedure is implemented in the Dataview NT software of TSI/Aerometrics.

The phase ratio based discrimination is also improved upon by implementing the half-integer phase ratio that is shown to be particularly effective in eliminating the large reflecting particles, which may otherwise appear as small refracting particles.

Droplet path lengths are used to determine the effective dimensions of the probe volume. Two methods—based on the second moment and the mode of the path length distribution—are examined. The mode-based method is found to be more reliable in practical situations.

Preliminary experimental results are reported to support the above concepts.

# 1. INTRODUCTION

In a highly dense spray, such as a rocket fuel injector, the phase Doppler probe volume needs to be focused very strongly, in order to eliminate the probability of multiple drops in the probe volume. This leads to a probe volume that may be substantially smaller than the largest drop being measured, as shown in the work by Strakey et al. (1998). Under these conditions, particle trajectory effects are strong and the conventional methods of probe volume correction are not applicable. However, accurate particle size and mass flux measurements can be obtained by using a combination of techniques, as listed below:

1.  *Pedestal amplitude (intensity) measurement*: Certain particle trajectories result in signals dominated by reflection as opposed to refraction. In general, the reflection-based signals are weak and make small particles appear large, and vice versa. By setting upper and lower thresholds on the signal pedestal height (also referred to as "intensity validation" in work by Bachalo, 1991), most of these signals can be rejected. Intensity validation is particularly helpful in rejecting small particles that would be otherwise detected as large particles and would cause serious errors in the mass flux measurement.

2.  *Half-integer phase ratio*: Two phase shift signals measured on each particle can be very effective in rejecting the reflection-based signals, provided that the ratio of larger-to-smaller phase shift is a half-integer. The phase Doppler receiver was modified to obtain a phase ratio of about 3.5, instead of the conventional value of 3.

3.  *Modified probe volume correction*: The effective size of the probe volume is known to increase with increasing particle size. A comprehensive review of this can be found in work by Bachalo et al. (1991) and Saffman (1987). One must remember, however, that the effective probe volume size cannot be assumed to increase with droplet size if intensity validation is implemented. The upper and lower intensity thresholds define the width of the probe volume. So, the actual width of the probe volume is smaller than or equal to the width defined by the intensity limits. This fact is taken into consideration in the modified probe volume correction procedure.

Development work on the above enhancements of the phase Doppler technique is reported in this paper. The phase Doppler based mass flux is compared with the measured data based on a mechanical patternator.

## 2. QUALIFICATION OF SMALL PROBE VOLUMES

Special care is needed in designing phase Doppler optics that are used to generate a small probe volume at a large standoff (probe-to-measurement point distance). The focused spot size cannot be deduced reliably from the theoretical Gaussian beam calculations.

We have set up engineering design procedures to obtain desirable probe volume sizes. Moreover, after assembly and alignment, each probe is qualified experimentally using a CCD-based laser beam profiler. A typical profile is shown in Figure 1, which corresponds to a laser spot with $1/e^2$ dimension of 58.0 $\mu$m.
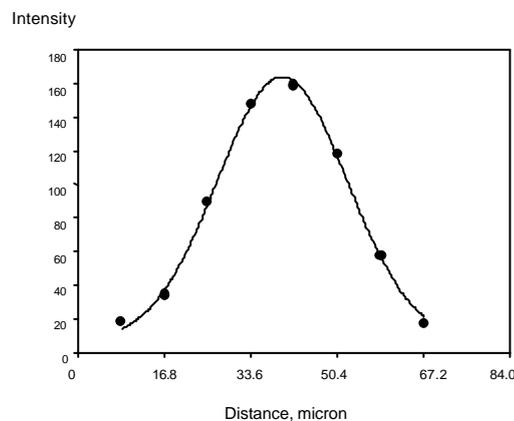


Figure 1: Linear profile of the probe volume with a Gaussian fit

Accurate information about the probe volume dimensions is important for precise mass flux measurement.

## 3. PARTICLE TRAJECTORY EFFECTS AND INTENSITY VALIDATION

A conventional case of the particle trajectory effect is illustrated in Figure 2. The drop trajectories are nearly perpendicular to $yz$-plane. It is clear that the nature of drop illumination changes drastically with the location of the drop along the $y$-axis.
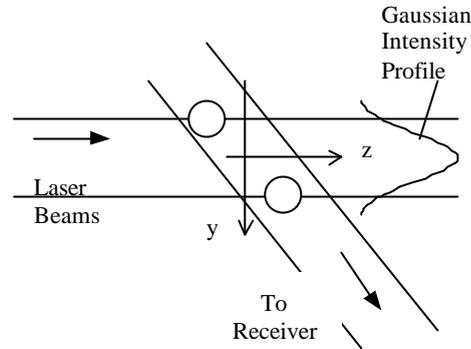


Figure 2: Particle location and Gaussian profile

If the drop trajectory is on the positive side of the $y$-axis, the backside of the drop (relative to the receiver) has stronger illumination. Hence, refracted light has a strong contribution to the collected signal, which is desirable if the system calibration is based on refraction.

On the other hand, when the drop trajectory intersects the measurement volume with a negative $y$-coordinate, the front side of the drop is more strongly illuminated and reflected light becomes strong, which leads to undesirable changes in the measured phase shift if the system calibration is based on refraction.

The transition from refraction to reflection is gradual when the drop diameter is large but not larger than the measurement volume diameter. In the present application, the drop diameters can be several times larger than the measurement volume.

As illustrated in Fig. 3, a very large drop sends refracted light in the direction of the receiver only when the center of the drop (shown with solid line) is at a certain range of locations on the positive $y$-axis. Similarly, only a small range of locations on the negative $y$-axis results in reflected light reaching the receiver. At other locations, both reflected and refracted light rays fail to reach the receiver. It is interesting to note that a large particle would not generate a signal when it is centered on the measurement volume.
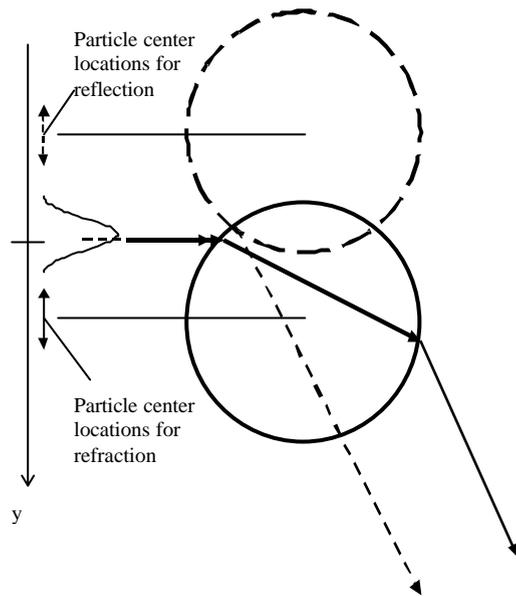
Figure 3: Scattering by a particle larger than the beam waist size

The above phenomena are explored using simulations based on generalized Lorenz-Mie theory by Gréhan et al. (1994). The results are presented and discussed below.

The amplitudes and phase shifts of signals for two different drop diameters are shown in Fig. 4. The values of $x$ and $z$ coordinates are zero for these computations and $y$ is changed in increments of 10 µm. The probe volume diameter is 60 µm and the receiver is located at a 30° off-axis angle. The phase ratio between the two detector pairs (1-3 and 1-2) is nearly 3 (a phase ratio of 3.5 is considered in Sec. 4).

As expected, the regions of refracted and reflected signals are well separated for a 100 µm drop. The strongest signals are obtained when the drop center is about 40 µm away from the center of the measurement volume along the positive $y$-axis.
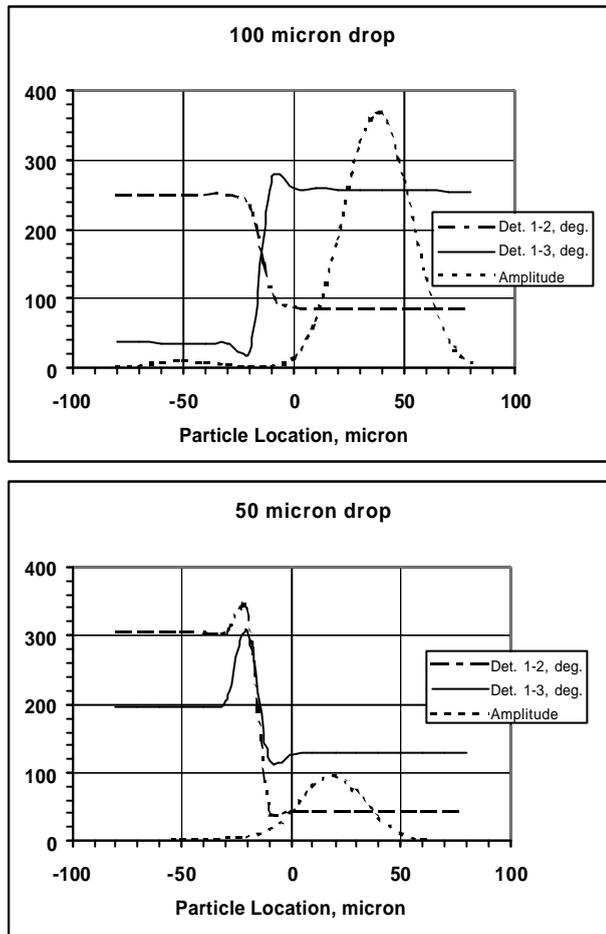
Figure 4: Amplitude and phase response as a function of *y*-location

The peak on the positive *y*-axis pertains to dominant refraction and leads to correct size measurement. The corresponding values of phase shift between detector pair 1-3 and 1-2 are 258° and 88° respectively. As shown in Fig. 5, they represent the correct ratio of phase shift for refraction, represented by the dotted line.

The reflection based phase values generated by a 100 µm drop are about 38° and 251° for the detector pairs 1-3 and 1-2 respectively. According to Fig. 5 this phase angle pair is also associated with a valid drop size (about 285 µm). Hence, comparison of phase shifts would *not* be effective in rejecting these erroneous signals.
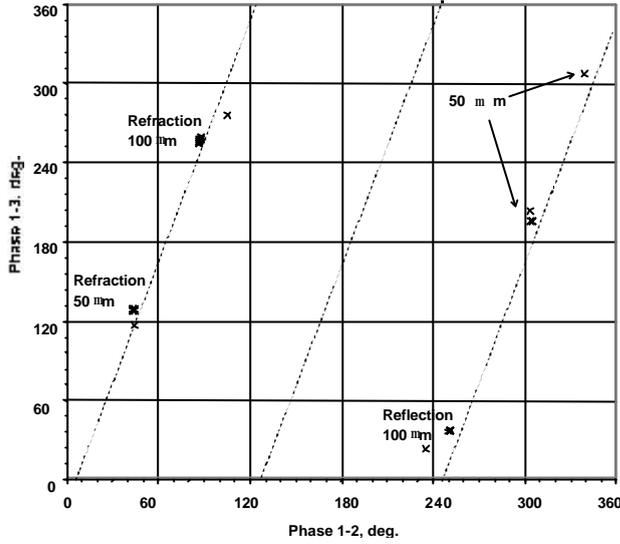
Figure 5: Comparison of the two phase-difference signals

If 10:1 limits are applied to signal peak amplitudes, all the signals appearing as 100 µm and having amplitude smaller than 37 units in Fig. 4 will be rejected. All the valid signals will correctly represent the drop size and will originate from an effective measurement volume, whose width can be expressed as

$$W_c = d_{mv} \sqrt{\frac{1}{2} \ln\left(\frac{1}{g}\right)},$$  (1)

where $d_{mv}$ is the $1/e^2$ measurement volume diameter and $g$ is the ratio of lower-to-upper amplitude limits.

In the present case, the intensity based probe volume width is 64 µm.

All the 100 µm drops that appear to be 285 µm due to reflection will be rejected as their amplitudes are too small. For a 285 µm drop, the valid signal must have an amplitude of at least 300 ($= 37 \times 285^2/100^2$) units.

In the case of 50 µm drops, the phase data begins to deteriorate before the amplitude reaches 10% of the peak value. Hence, effective measurement volume is somewhat smaller than 64 µm. Some errors may be introduced by assuming the measurement volume to be fixed at 64 µm.

Again, reflection-based signals from a 50 µm drop result in a much larger measured diameter, and the ratio of the two phase shifts does not appear to be effective in discriminating these fictitiously large drops. However, amplitude discrimination will be very effective.

Amplitude discrimination may not be equally effective for large drops (larger than 200 µm) that would appear as small drops as a result of reflection. Firstly, it should be noted that this error would not cause any serious bias in the mass flux calculation. Secondly, it can be suppressed by using the half-integer phase ratio, as discussed in the following section.

## 4. HALF-INTEGER PHASE RATIO

A closer look at the phase ratio criterion shows that it is not a mere coincidence that reflection based signals from both 50 and 100 µm drops are recognized as valid particles (see Fig. 5). In fact, the optical configuration of Sec. 3 will fail for all the drops in this respect, as explained below.

The phase shifts between refraction-based signals are positive and, starting at zero, increase with increasing drop diameter. The phase shift between detector pair 1-3 increases $r$ times faster than that between detector pair 1-2, where $r$ is the ratio of detector separation in each pair.

Similarly, phase shifts between reflection-based signals are negative and, starting at zero, decrease with increasing drop diameter. The phase shift between detector pair 1-3 decreases $r$ times faster than that

between detector pair 1-2. Since the signal processor is set up to look for positive phase shifts, the reflection-based signals appear to start at 360º for very small particles, as shown in Figs. 6 and 7.

Figure 6 shows a system with a nearly integer value of $r$ (i.e. ~3). In this case, there is always a refraction-based signal pair corresponding to a reflection-based pair and hence, all the reflection-based signals are prone to misinterpretation. The amplitude validation technique will reject the small drops appearing as large drops but would not be equally effective in identifying large drops that appear to be small.

The solution to this problem is simple. As shown in Fig. 7, a non-integer value of $r$ displaces the refraction based signals far from the reflection based signals, so that they can be identified and discarded. A half-integer value of $r$, such as 3½, is optimal for this purpose.
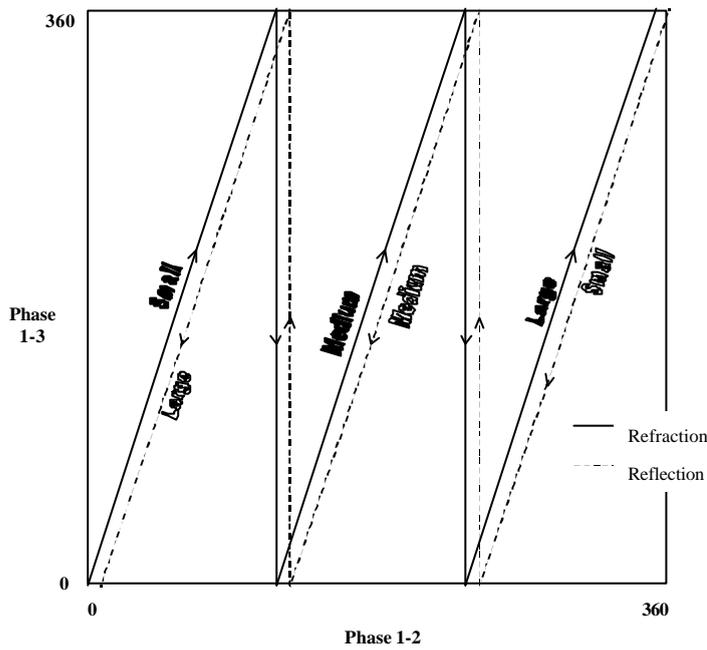


Figure 6: Reflection and refraction-based phase shifts for nearly integer ratio between phase signals; arrows indicate the direction of increasing diameters
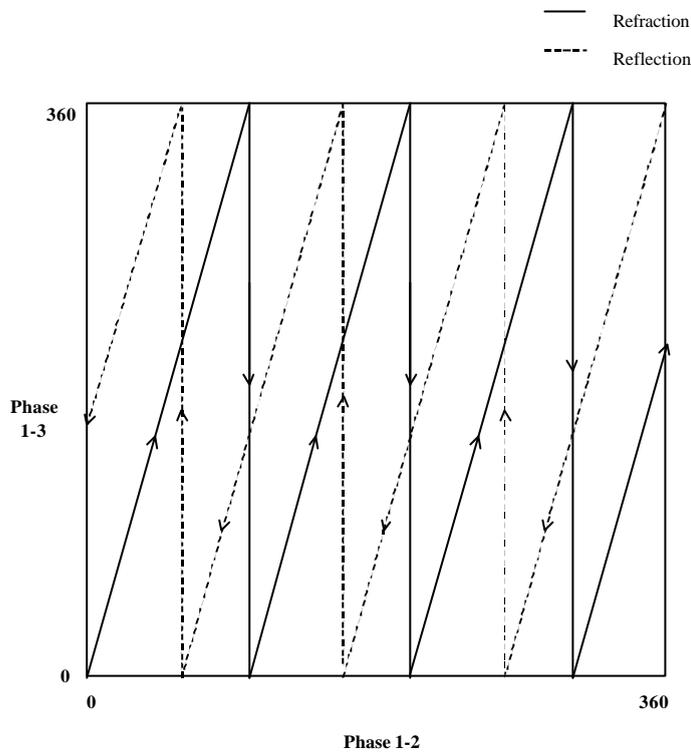
Figure 7: Reflection and refraction based phase shifts for non-integer ratio between phase signals; arrows indicate the direction of increasing diameters

The effectiveness of the half-integer phase ratio was tested by inverting the phase Doppler receiver and taking data. As shown in Fig. 8, the size histogram with correct receiver orientation represents a distribution with diameters up to 40 µm. This data was validated using ±7.56 µm tolerance (±2% of the overall size range that was 378 µm) on the diameters measured with Phase 1-2 and Phase 1-3. Upon inverting the receiver, the sign of Phase 1-2 and Phase 1-3 changes and they simulate the signals from reflecting particles. Now, Phase 1-2 and 1-3 yielded largely different diameter values and did not meet the above tolerance criterion, except for very small particles. The valid data rate with the inverted receiver was less than 0.5% of the original valid data rate and its contribution to mass flux was about 0.03%. In short, half-integer phase ratio is very effective in rejecting the large reflecting particles that may appear as small particles.
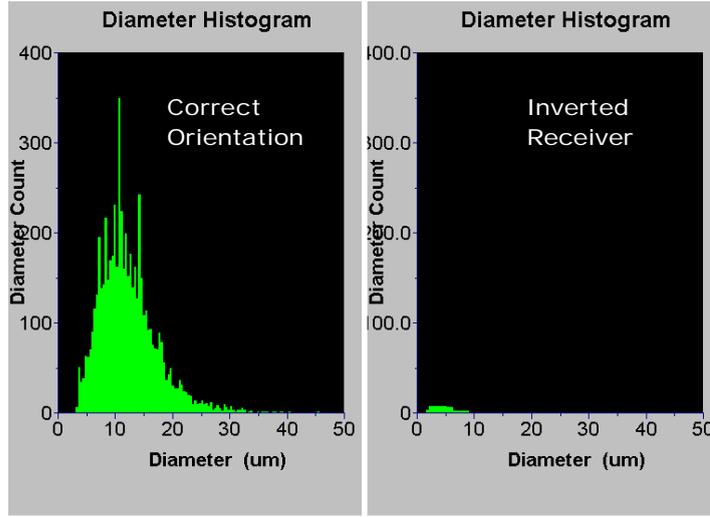
Figure 8: Size distributions for correct receiver orientation(left) and the inverted receiver(right)

## 5. MODIFIED PROBE VOLUME CORRECTION

In order to account for the increase of the probe volume width with the particle size, two procedures have been proposed. They are based on:

(i)    measurement of the square-mean path length of particles in a size bin (Saffman 1987);

(ii)   determination of the upper limit of path lengths in the size bin of interest (Bachalo et al. 1991).

Procedure (i) counts on the path length $\ell$ to follow an idealized distribution function that is based on a circular probe volume cross-section and uniformly distributed particle trajectories. This function is not reported explicitly in literature. Nonetheless it can be derived by considering the path length at a certain y-location. As shown in Fig. 9,

$$\ell = \sqrt{\ell_{\max}^2 - 4y^2} \ . \tag{2}$$

The probability that the path length lies between $\ell$ and $\ell + d\ell$ is proportional to the corresponding value of $|dy|$. Hence, we need to differentiate Eq. (2), as follows:

$$d\ell = -4\left(\ell_{\max}^2 - 4y^2\right)^{-1/2} y \, dy \ . \tag{3}$$

Eliminating $y$ using Eq. (2), the path length distribution may then be expressed as

$$p(\ell) = \left|\frac{dy}{d\ell}\right| = \frac{\ell}{2\sqrt{\ell_{\max}^2 - \ell^2}} \ . \tag{4}$$
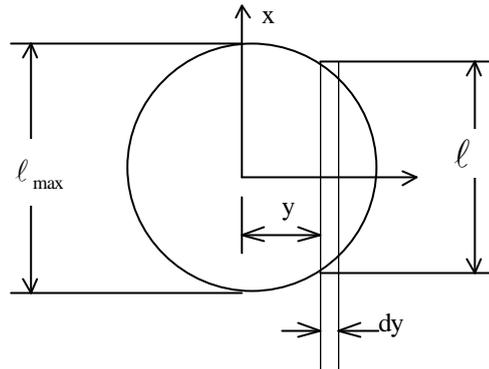
Figure 9: Probe volume geometry for derivation of the path-length distribution

Real path length distributions may vary significantly from this function due to various reasons. Some measured path length distributions are shown in Fig. 10. Quite clearly, Eq. (4) is not a very good fit for these distributions. However, a peak path length can be deduced from these data and used as a measure of the probe volume width. The most reliable results were obtained by using the 95% point of the cumulative path length distribution as the nominal upper limit.
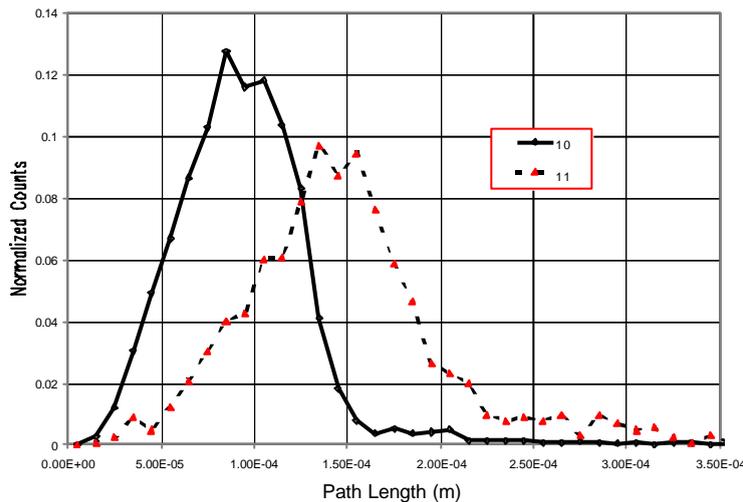


Figure 10: Path length distributions for 22.5 µm drops and PMT voltages of 350 and 500 V
(Run # 10 & 11)

As mentioned above, using intensity validation results in an upper limit being imposed on the effective probe volume width beyond a certain drop diameter. For very small particles, path length based probe volume width is smaller than the width based on the intensity limits ($W_c$). It gradually increases with increasing particle size and reaches $W_c$. Beyond this point, $W_c$ is used as the probe volume width for the purpose of probe volume correction and mass flux calculations.

## 6. EXPERIMENTAL RESULTS

In order to verify the above tools for probe volume correction and mass flux calculation, preliminary measurements were conducted in a moderately dense air-blast spray using a strongly focused probe volume. The spray had a circular cross-section and was fairly symmetric with $D_{20}$ varying from 28 µm at the center to 24 µm near the edges. Results of mass flux measurement are shown in Figure 11. Assuming radial symmetry, the total flux was computed to be 1.57 cc/sec. In the absence of a reliable mechanical

patternator, the total volume flow was estimated by collecting the spray liquid over a known time interval. This measurement indicated a flow rate of 1.44 cc/sec. Considering that some liquid escaped the collecting vessel in the form of a very fine mist, the agreement between phase Doppler and direct measurement is very good.
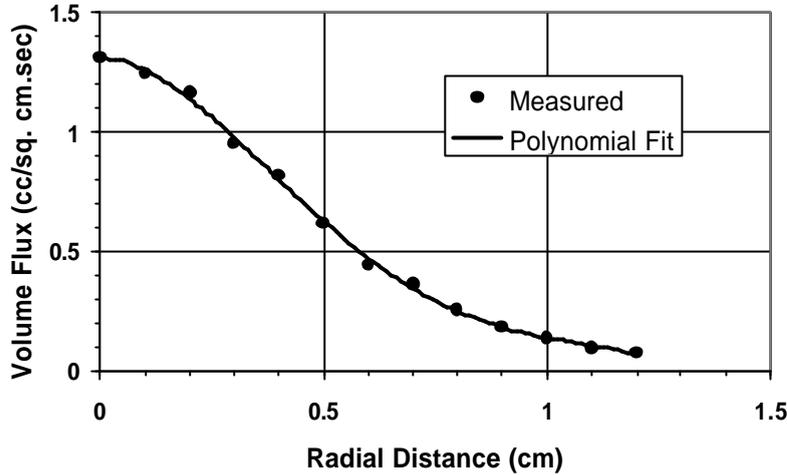
**Air Blast Nozzle**



Figure 11: Mass flux measurement using the present method

The phase Doppler results were also used to estimate the attenuation of a laser beam through the spray as follows:

$$\frac{P_{out}}{P_{in}} = \exp\left[-\frac{p}{2}\left(\sum_i D_{20i}^2 C_i L_i\right)\right], \tag{5}$$

where $D_{20i}$, $C_i$ and $L_i$ are the area-mean diameter, the number concentration and the path length associated with the $i$th point along a linear path. Along a radial path 2" below the nozzle the attenuation was estimated to be 0.85. This result compared well with a direct measurement of 0.83 using a He-Ne laser beam.

## 7. CONCLUSION

Several modifications are incorporated in the conventional phase Doppler system to enable accurate size distribution and mass flux measurements in a dense spray. The problem of trajectory effect is completely resolved for arbitrary combinations of drop size and probe volume diameter, including the case of probe volumes being much smaller than the drop sizes. In this process, a portion of refraction based signals are also rejected, but the remaining signals are free of sizing errors and correspond to a well-defined region in space. The software algorithms for these modifications have been coded and incorporated into a Windows NT based phase Doppler system software (Dataview™ NT, TSI/Aerometrics Inc.). Determination of intensity limits and the corresponding probe volume correction procedure are fully automated.

## REFERENCES

Bachalo, W. D. (1991) "Method for measuring the size and velocity of spherical particles using the phase and intensity of scattered light", US Patent # 4986659

Bachalo, W. D., Breña de la Rosa, A. and Sankar, S. V. (1991) "Diagnostics for fuel spray characterization", Chapter 7, Combustion Measurements, Ed: N. Chigier, Hemisphere Publishing Corporation, 1991

Gréhan, G., Gouesbet, G. Naqwi, A. and Durst, F. (1994) "Trajectory ambiguities in phase Doppler systems: study of a near-forward and a near-backward geometry," Particle and Particle System Characterization 11, pp. 133–144.

Saffman, M. (1987) "Automatic calibration of LDA measurement volume size", Applied Optics, 26, pp. 2592-2597

Strakey, P. A., Talley, D. G., Sankar, S. V. and Bachalo, W. D. (1998) "The use of small probe volumes with phase Doppler interferometry", Proc. ILASS-Americas '98, Sacramento, CA

## ACKNOWLEDGEMENT